

A Mechanistic Study of the Alkaline Hydrolysis of Diaryl Sulfate Diesters

Jarod M. Younker and Alvan C. Hengge*

Utah State University, Department of Chemistry and Biochemistry, 0300 Old Main Hill,
Logan, Utah 84322-0300

hengge@cc.usu.edu

Received July 10, 2004

Nearly all of the reported studies of reactions of sulfate diesters are for dialkyl or alkyl aryl diesters, which undergo reaction by carbon–oxygen bond fission. Sulfuryl transfer reactions of sulfate diesters (RO–SO₂–OR') proceeding by attack at sulfur have been little explored. When both ester groups are aryl groups the hydrolysis reaction (sulfuryl transfer to water) occurs by way of attack at sulfur. The alkaline hydrolysis of diaryl sulfate diesters was shown to obey first-order kinetics with respect to [OH⁻] and proceed through S–O bond fission, in a mechanism that is most likely concerted. Activation parameters for 4-chloro-3-nitrophenyl phenyl sulfate and 4-nitrophenyl phenyl sulfate gave the following respective values: $\Delta H^\ddagger = 88.0 \pm 0.1$ and 84.83 ± 0.06 kJ mol⁻¹ and $\Delta S^\ddagger = -37 \pm 1$ and -50.2 ± 0.5 J mol⁻¹ deg⁻¹. The dependence of the second-order rate constant for hydrolysis on leaving group pK_a was analyzed giving a β_{lg} slope of -0.7 ± 0.2 and a Leffler α parameter value of 0.36. A ¹⁵k kinetic isotope effect (KIE) for the hydroxide attack on 4-nitrophenyl phenyl sulfate of 1.0000 ± 0.0005 and an ¹⁸k_{lg} KIE value of 1.003 ± 0.002 were obtained.

Introduction

Sulfate monoesters, like phosphate esters, are of interest due to their biological importance, and in the laboratory, sulfate diesters have found considerable utility as alkylating agents. Mechanistic studies incorporating linear free energy relationships (LFERs), activation parameters, and kinetic isotope effects (KIE) data have been reported for sulfate monoesters, for aryl sulfuryl chlorides, and for alkyl aryl sulfate diesters, but little is known about the reactions of diaryl sulfate diesters.¹ Activation parameters, ¹⁸O-tracer studies, LFER, and KIEs of diaryl sulfate diesters were measured in this work in order to shed light on the mechanism of the alkaline hydrolysis reactions of these sulfate diesters.

Previous studies of the alkaline hydrolysis of sulfate monoesters in the pH-independent range of 4–12^{2–6} have shown the following: alkyl sulfate monoesters undergo C–O bond fission;⁷ the 4-nitrophenyl sulfate monoester anion undergoes hydrolysis by S–O bond fission, except at pH > 12, where competitive attack of hydroxide on

the aromatic ring with aryl–O bond fission also occurs;^{3,8} aryl sulfuryl chlorides undergo both S–O and S–Cl bond fission;^{9,10} alkyl aryl sulfate diesters undergo alkyl–O bond fission.^{11,12} It has also been shown that the alkaline hydrolysis of diphenyl sulfate leads to the formation of phenol and the phenyl sulfate monoester.¹ To our knowledge, no further mechanistic studies of diaryl sulfate diesters have been reported.

For the hydrolysis of aryl sulfate monoesters, a concerted mechanism with a loose transition state and little nucleophilic participation is supported by both LFER^{2,3,13–15} and KIEs.^{6,16} Sulfuryl transfer of phenyl [(R)¹⁶O,¹⁷O,¹⁸O]-sulfate to a secondary alcohol proceeds with inversion of configuration,¹⁷ ruling out SO₃ as a freely diffusible intermediate. These conclusions are similar to those for the hydrolysis of phosphate monoesters. If the effect of a second alkylation on the mechanism of sulfuryl transfer is similar to that for phosphoryl transfer, then the transition state for sulfuryl transfer in a diester is expected to become tighter (more associative). LFER

* To whom correspondence should be addressed. Fax: 435-797-3390.

(1) Kaiser, E. T.; Katz, I. R.; Wulfers, T. F. *J. Am. Chem. Soc.* **1965**, *87*, 3781–3782.

(2) Fendler, E. J.; Fendler, J. H. *J. Org. Chem.* **1968**, *33*, 3852–3859.

(3) Benkovic, S. J.; Benkovic, P. A. *J. Am. Chem. Soc.* **1966**, *88*, 5504–5511.

(4) Bethell, D.; Fessey, R. E.; Engberts, J. B. F. N.; Roberts, D. W. *J. Chem. Soc., Perkin Trans. 2* **2001**, 1496–1502.

(5) Bethell, D.; Fessey, R. E.; Namwindwa, E.; Roberts, D. W. *J. Chem. Soc., Perkin Trans. 2* **2001**, 1489–1495.

(6) Burlingham, B. T.; Pratt, L. M.; Davidson, E. R.; Shiner, V. J. J.; Fong, J.; Widlanski, T. S. *J. Am. Chem. Soc.* **2003**, *125*, 13036–13037.

(7) Kaiser, E. T.; Panar, M.; Westheimer, F. H. *J. Am. Chem. Soc.* **1963**, *85*, 602–607.

(8) Spencer, B. *Biochem. J.* **1958**, *69*, 155–159.

(9) Buncel, E.; Raoult, A. *Can. J. Chem.* **1972**, *50*, 1907–1911.

(10) Buncel, E.; Raoult, A.; Lancaster, L. A. *J. Am. Chem. Soc.* **1973**, *95*, 5964–5967.

(11) Buncel, E.; Chuaqui, C. *J. Org. Chem.* **1980**, *45*, 2825–2830.

(12) Buncel, E.; Raoult, A.; Wiltshire, J. F. *J. Am. Chem. Soc.* **1973**, *95*, 799–802.

(13) Hopkins, A.; Day, R. A.; Williams, A. *J. Am. Chem. Soc.* **1983**, *105*, 6062–6070.

(14) D'Rozario, P.; Smyth, R. L.; Williams, A. *J. Am. Chem. Soc.* **1984**, *106*, 5027–5028.

(15) Bourne, N.; Hopkins, A.; Williams, A. *J. Am. Chem. Soc.* **1985**, *107*, 4327–4331.

(16) Hoff, R. H.; Larsen, P.; Hengge, A. C. *J. Am. Chem. Soc.* **2001**, *123*, 9338–9344.

(17) Chai, C. L. L.; Hepburn, T. W.; Lowe, G. *J. Chem. Soc., Chem. Commun.* **1991**, *19*, 1403–1405.

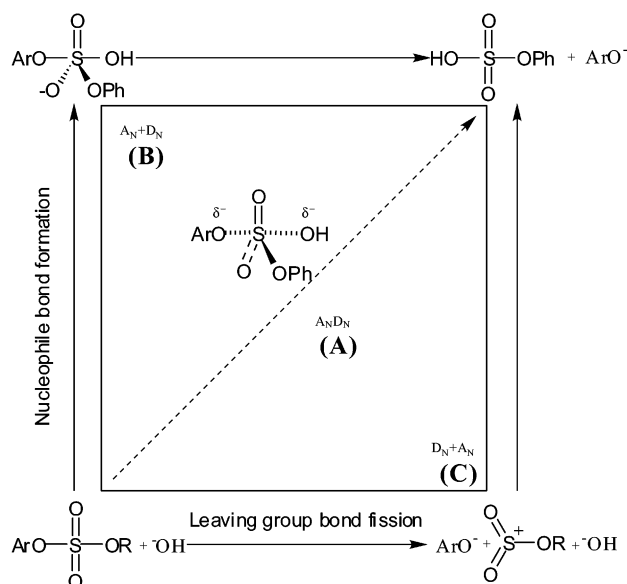


FIGURE 1. More–O’Ferrall Jencks diagram outlining the mechanistic possibilities for the alkaline hydrolysis of a diaryl sulfate diester. The products shown would rapidly undergo proton transfer to form PhOSO_3^- and ArOH .

studies on sulfonyl group transfer between compounds of the form $\text{R-SO}_2\text{-OAr}$ and aryl oxide nucleophiles support synchronous, concerted reactions for nucleophiles and leaving groups with $\text{p}K_a$ values in the range 7–10.¹⁸ Since sulfate diesters with an alkyl group undergo reaction by alkyl–O bond fission, the study here affords the first examination of the mechanism of sulfuryl transfer in diesters ($\text{RO-SO}_2\text{-OR'}$) proceeding by attack at sulfur.

Excluding attack at the aryl carbon, Figure 1 shows three possible mechanisms for the hydrolysis of diaryl sulfate diesters illustrated in a More–O’Ferrall–Jencks diagram. The abscissa and ordinate axes indicate the degree of leaving group bond fission and nucleophile bond formation, respectively; the reactants are in the lower left corner, products in the upper right. Mechanism **A** represents a synchronous, concerted mechanism, designated $\text{A}_\text{N}\text{D}_\text{N}$ in the IUPAC nomenclature,¹⁹ wherein leaving group departure and nucleophilic attack progress linearly (i.e., the sum of the bond order to nucleophile and leaving group = 1). Mechanism **B** is a two-step mechanism ($\text{A}_\text{N} + \text{D}_\text{N}$) where a pentacoordinate intermediate is formed, followed by leaving group departure; which step is rate-limiting will depend on the relative $\text{p}K_a$ values of the entering and leaving groups. Mechanism **C** ($\text{D}_\text{N} + \text{A}_\text{N}$) also involves two steps, with leaving group dissociation proceeding first, with formation of an intermediate, followed by nucleophile attack in a second step. In this mechanism the first step should be rate-limiting.

Results and Discussion

The following series of diaryl sulfate diesters were synthesized from phenyl sulfonyl chloride (**1**) and the

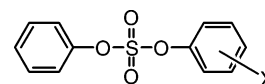


FIGURE 2. Representative diaryl sulfate; X = variable substituent as defined in Table 1.

TABLE 1. List of Diaryl Sulfate Diesters with Leaving Groups and Their $\text{p}K_a$ Values

compd	leaving group (phenol)	leaving group $\text{p}K_a$
2	4Cl-3- NO_2	7.75 ²⁰
3	4- NO_2	7.15 ²¹
4	2,6- F_2	7.12 ²²
5	2-F-4- NO_2	6.2 ²³
6	2,3,4,5,6- F_5	5.33 ²²
7	3-F-4- NO_2	5.3 ²³

appropriate phenol: 4-chloro-3-nitrophenyl phenyl sulfate (**2**), 4-nitrophenyl phenyl sulfate (**3**), 2,6-difluorophenyl phenyl sulfate (**4**), 2-fluoro-4-nitrophenyl phenyl sulfate (**5**), pentafluorophenyl phenyl sulfate (**6**), and 3-fluoro-4-nitrophenyl phenyl sulfate (**7**). Figure 2 shows a representative diaryl sulfate diester, and Table 1 gives the aryl leaving groups with their respective $\text{p}K_a$ values.

To determine the position of bond fission, the reaction of **4** was carried out in water containing 32% H_2^{18}O . GC–MS analysis of recovered 2,6-difluorophenol showed no ^{18}O incorporation (see the Supporting Information). FTIR of the recovered barium phenyl sulfate showed the presence of ^{18}O incorporation ($\nu_1 [\text{S}^{16}\text{O}_3^{18}\text{O sym}] = 964 \text{ cm}^{-1}$, $\nu_1 [\text{S}^{16}\text{O}_4 \text{ sym}] = 984 \text{ cm}^{-1}$, see the Supporting Information). This result shows that within the limits of detection, the alkaline hydrolysis reaction proceeds by S–O bond fission. Compounds **3**, **5**, and **7** could not be used in the ^{18}O -tracer study due to the documented oxygen exchange of the phenolic oxygen atom with hydroxide under alkaline conditions of phenols substituted with either a 2- or a 4-nitro group.²⁴

The hydrolysis of **3** was followed by HPLC to ascertain whether 4-nitrophenolate and phenyl sulfate were the only products. The hydrolysis of **3** at 1, 2, and 3 half-lives yielded, as products, 88 ± 1 , 85 ± 3 , and $92 \pm 1\%$ 4-nitrophenol and 12 ± 1 , 15 ± 3 , and $9 \pm 1\%$ phenol, respectively. Hydrolysis of phenyl sulfate under identical conditions showed only trace amounts of phenol, indicating that the phenol found after the hydrolysis of **3** did not result from subsequent hydrolysis of the phenyl sulfate monoester product but, rather, from primary hydrolysis of the diester. Thus, loss of the better leaving group, 4-nitrophenolate, accounts for $\sim 90\%$ of the reaction pathway for **3**. While an even larger preponderance of this pathway might be expected on the basis of the difference in $\text{p}K_a$, this result echoes the chemistry of aryl sulfonyl chlorides, where loss of the aryl group was found to be competitive with loss of chloride.^{9,10}

The hydrolysis of the diesters in Table 1 were followed by monitoring a wavelength characteristic of the better

(20) Hunter, A.; Renfrew, M.; Rettura, D.; Taylor, J. A.; Whitmore, J. M. J.; Williams, A. *J. Am. Chem. Soc.* **1995**, *117*, 5484–5491.

(21) Fickling, M. M.; Fischer, A.; Mann, B. R.; Packer, J.; Vaughan, J. *J. Am. Chem. Soc.* **1959**, *81*, 4226–4230.

(22) Stefanidis, D.; Cho, S.; Dhe-Paganon, S.; Jencks, W. P. *J. Am. Chem. Soc.* **1993**, *115*, 1650–1656.

(23) Chapman, E.; Bryan, M. C.; Wong, C. H. *Proc. Natl. Acad. Sci. U.S.A.* **2003**, *100*, 910–915.

(24) Hengge, A. C. *J. Am. Chem. Soc.* **1992**, *114*, 2747–2748.

(18) Williams, A. *Adv. Phys. Org. Chem.* **1992**, *27*, 1–55.

(19) Guthrie, R. D.; Jencks, W. P. *Acc. Chem. Res.* **1989**, *22*, 343–349.

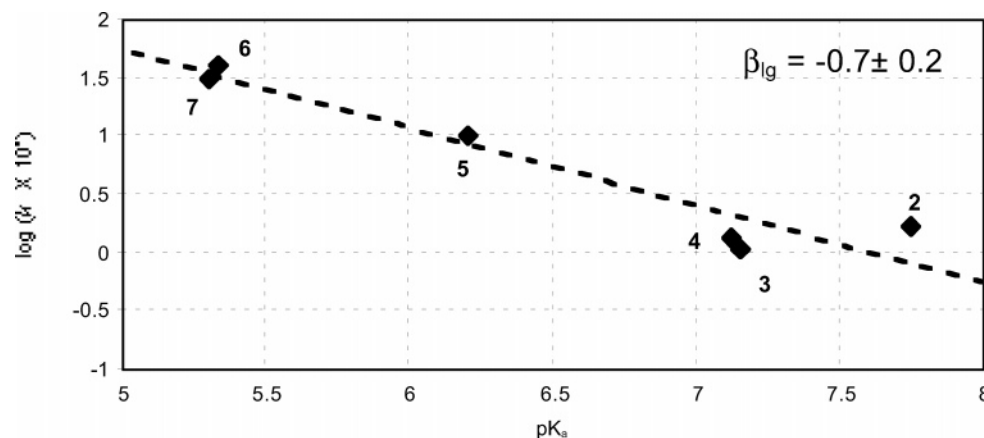


FIGURE 3. Log of the second-order rate constant k_{OH} ($\times 10^4$) for hydroxide attack on compounds **2–7** plotted as a dependent function of the $\text{p}K_{\text{a}}$ of the leaving group, giving a slope (β_{lg}) of -0.7 ± 0.2 .

TABLE 2. Activation Parameters

	ΔH^\ddagger (kJ mol $^{-1}$)	ΔS^\ddagger (J mol $^{-1}$ deg $^{-1}$)
compd 2	88.0 ± 0.1	-37 ± 1
compd 3	84.83 ± 0.06	-50.2 ± 0.5

TABLE 3. Brønsted Data and Effective Charges

$\epsilon_{\text{reactant}}$	$\epsilon_{\text{product}}$	β_{eq}	β_{lg}	α
$0.83 \pm 0.07^{b,25}$	-1.00 ± 0.00	-1.83 ± 0.07	-0.7 ± 0.2	0.36

^b Published value for an aryl alkylsulfonate.

leaving group (i.e., 400 nm for **3**) to obtain the rates of the predominant reaction pathway for each compound. The hydrolyses of all compounds **2–7** were first-order in hydroxide concentration (see the Supporting Information). Therefore, the $\text{D}_{\text{N}} + \text{A}_{\text{N}}$ mechanism **C** can be ruled out, as the dissociation of the sulfate diester should be rate limiting and the rate would be independent of nucleophile concentration.

Rates were measured from 30 to 60 °C to obtain the activation parameters for compounds **2** and **3**, which are given in Table 2. The values for ΔH^\ddagger and ΔS^\ddagger are as expected for a bimolecular reaction in which a high energy, ordered transition state is observed. These parameters are consistent with either a concerted $\text{A}_{\text{N}}\text{D}_{\text{N}}$ mechanism or an associative $\text{A}_{\text{N}} + \text{D}_{\text{N}}$ mechanism.

The second-order rate constant for the alkaline hydrolysis of each diester was determined from the slope of the observed rate constant plotted as a dependent function of hydroxide concentration. The correlation between the second-order rate constants for hydroxide attack on the sulfate diesters on the $\text{p}K_{\text{a}}$ of the leaving group, yielding the Brønsted β_{lg} value of -0.7 ± 0.2 , is shown in Table 3 and Figure 3.

To date, a value for the effective charge (ϵ) on the aryl group in a sulfate diester has not been reported. The most structurally similar compound for which an effective charge has been reported is an aryl alkylsulfonate ($\text{R}-\text{SO}_2-\text{OAr}$), for which the effective charge on the aryl group is $+0.83 \pm 0.07$.²⁵ While this compound has one less atom with lone pairs bonded to the central sulfur, it is the closest neutral analogue for which an effective

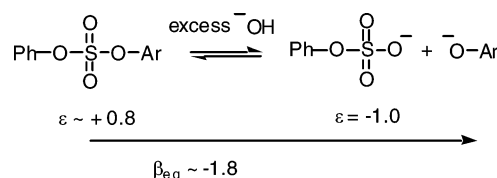


FIGURE 4. Definition of β_{eq} , the difference between the product effective charge, -1 , and the reactant effective charge, estimated at $+0.8$.

charge has been reported. For ionized aryl sulfate esters (ArOSO_3^-), which do share the characteristic of four oxygen atoms bonded to sulfur, $\epsilon = +0.7$,¹³ a very similar value. These values indicate that a reasonable estimate for the effective charge on the incipient leaving group in the reactant diesters is $\sim +0.8$. The difference between ϵ and the absolute charge of the expelled leaving group, -1 , gives a change in effective charge for the full reaction of ~ -1.8 , which is defined as β_{eq} (see Figure 4).¹⁸ The β_{lg} value of -0.7 for the hydrolysis of the compounds in Table 3 indicates that the effective charge on the leaving group changes from $+1.8$ in the reactant to $\sim +1.1$ in the transition state. The Leffler α parameter, indicating the fractional change in the leaving group effective charge in the transition state relative to the reactant, was determined as described in Williams ($\beta_{\text{lg}}/\beta_{\text{eq}}$).¹⁸ This Leffler constant of 0.36 indicates the leaving group has lost about one-third of its effective charge in the transition state of the rate-limiting step.

To supplement the information from the linear free energy relationship, KIEs were recorded at the positions indicated in Figure 5. The corresponding isotope effects have been measured for other group transfer reactions with the same leaving group. These include a number of reactions of 4-nitrophenyl acetate,²⁶ the hydrolysis of several phosphate esters, including 4-nitrophenyl phosphate monoester, and diesters, and triesters; and the hydrolysis of 4-nitrophenyl sulfate monoester.²⁷ The primary isotope effect $^{18}\text{k}_{\text{bridge}}$ gives a measure of the degree of bond fission to the leaving group in the transition state. Its maximum value with the 4-nitro-

(25) Deacon, T.; Farrar, C. R.; Sikkil, B. J.; Williams, A. J. *Am. Chem. Soc.* **1978**, *100*, 2525–2534.

(26) Hengge, A. C.; Hess, R. A. *J. Am. Chem. Soc.* **1994**, *116*, 11256–11263.

(27) Hengge, A. C. *Acc. Chem. Res.* **2002**, *35*, 105–12.

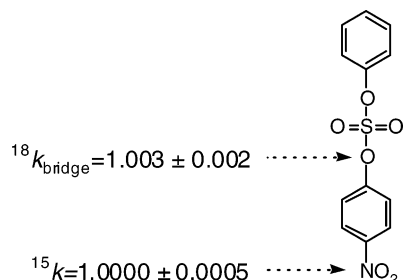


FIGURE 5. Compound (**3**) with sites of KIE determination indicated.

phenyl leaving group is in the range 1.02–1.03 in a late transition state with significant bond fission, such as the hydrolysis of 4-nitrophenyl sulfate and 4-nitrophenyl phosphate.²⁷ In hydrolysis reactions of phosphodiester, which are concerted with tighter transition states and less bond fission to the leaving group, $^{18}k_{\text{bridge}}$ ranges from 1.004 to 1.006.²⁷ The isotope effect in the nitrogen atom, ^{15}k , is a measure of the degree of negative charge delocalized into the nitro group.²⁷ This isotope effect arises from contributions from a quinonoid resonance form in the nitrophenolate anion, and differences in stiffness of N–O bonds and N–C bonds. Because N–O bonds are stiffer, the nitrogen atom is more tightly bonded in neutral 4-nitrophenol than in the phenolate anion. The ^{15}K EIE for deprotonation of 4-nitrophenol is thus normal, 1.0023 ± 0.0002 .²⁸

The small $^{18}k_{\text{bridge}}$ of 1.003 for the hydrolysis of 4-nitrophenyl phenyl sulfate suggests a small degree ($\sim 10\%$) of bond fission in the transition state. Consistent with this, the unity value for ^{15}k indicates no significant negative charge development. Yet, the Brønsted β_{lg} value of -0.7 indicates that the leaving group experiences a significant change in “effective” charge in the transition state. An event other than bond fission that could result in such a change is progress toward formation of a pentacoordinate intermediate as a result of nucleophilic attack. In such a species, the sulfonyl group will be less electrophilic and impart a reduced “effective” charge on the leaving group. Analogous effects are well-known in carbonyl chemistry, where the hyperconjugation of α -hydrogen atoms is reduced or abolished upon partial (transition state) or full (equilibrium) conversion of a carbonyl to a tetrahedral species. Similarly, significant negative values for β_{acyl} (-2.0 to -2.5) have been reported for reactions of substituted 4-nitrophenyl benzoates ($4\text{-X-C}_6\text{H}_4\text{C(O)-OC}_6\text{H}_4\text{-4-NO}_2$) with various nucleophiles.²⁹

A fully formed, pentacoordinate sulfur intermediate need not form in the present reaction, and there is no evidence for such a species in the present study. If a true intermediate were to form, its formation should be rate-limiting, since expulsion of the leaving group ($\text{p}K_{\text{a}}$ 7.15 in the case of **2**) is much more favorable than expulsion of hydroxide ($\text{p}K_{\text{a}}$ 15.7) to revert to the reactants. Such a mechanism would exhibit KIEs for formation of the intermediate; this should give rise to a small inverse value for $^{18}k_{\text{bridge}}$ due to the compression of bending modes

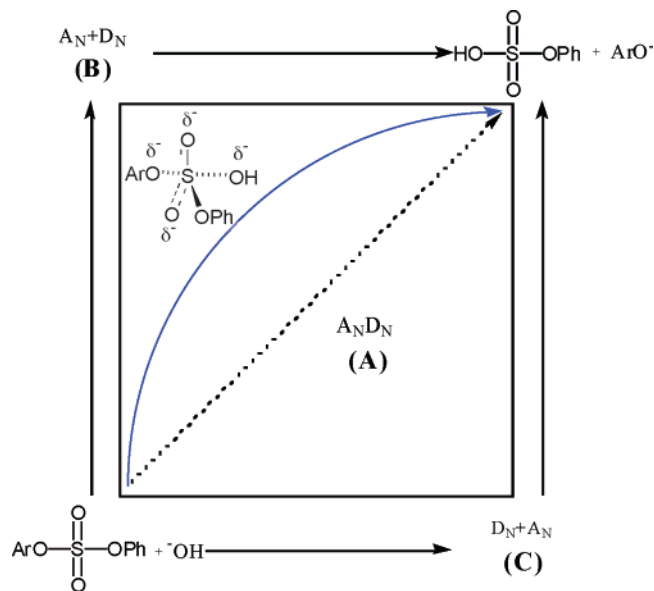


FIGURE 6. More–O’Ferrall Jencks diagram showing the proposed mechanism for diaryl sulfate hydrolysis (blue curved arrow). Although the reaction is most likely concerted, nucleophilic addition is more advanced than leaving group bond fission.

in the pentacoordinate intermediate. Precedence for this has been observed in the amide- ^{15}N isotope effect for the alkaline hydrolysis of 4-nitroanilide.³⁰ Under conditions where formation of a tetrahedral intermediate is rate-limiting, $^{15}k = 0.995$, in contrast to $^{15}k = 1.035$ when breakdown of the tetrahedral intermediate is rate-limiting.³⁰ Knowledge of the β_{nuc} value in order to cross-correlate β_{nuc} with β_{lg} would have shed further insights into this reaction; however, an attempt to measure β_{nuc} for a series of phenoxide nucleophiles was not successful, as these nucleophiles showed no measurable reaction toward 4-nitrophenyl phenyl sulfate at 40 °C.

Conclusions

The combination of the KIE and LFER data are most easily explained by a concerted mechanism with a tight transition state, in the upper left region of the More–O’Ferrall–Jencks diagram (Figure 6). In such a transition state, nucleophilic bond formation is more advanced than leaving group bond fission. Nucleophilic attack must have proceeded to a greater extent than leaving group departure in the transition state to give the combination of a significant Leffler α and small $^{18}k_{\text{bridge}}$ and ^{15}k values. The fact that $^{18}k_{\text{bridge}}$ is not inverse argues against nucleophilic attack in a step preceding leaving group departure, which would form a pentacoordinate intermediate in the rate-limiting step. The disparity between the very small isotope effects in the leaving group and the Leffler α constant most likely arises from a change in effective charge resulting from the sulfonyl group accepting, to a degree, the donated nucleophile electrons before totally transferring the resultant charge to the leaving group. This interpretation is in agreement with the ability of the neutral sulfate reactant to accept electron density, especially in comparison with the

(28) Hengge, A. C.; Cleland, W. W. *J. Am. Chem. Soc.* **1990**, *112*, 7421–7422.

(29) Um, I.-H.; Jeon, J.-S.; Kwon, D.-S. *Bull. Korean. Chem. Soc.* **1991**, *12*, 406–410.

(30) Hengge, A. C.; Stein, R. L. *Biochemistry* **2004**, *43*, 742–7.

charged phosphate diester, accounting for the low sulfate diester $^{18}k_{\text{bridge}}$ that is at the lower end of the $^{18}k_{\text{bridge}}$ values seen for concerted phosphate diester reactions.

The related aryl sulfonates have been shown to react by attack at sulfur in a concerted mechanism;^{14,15,25} for the present compounds, the significant negative value of β_{lg} , KIEs, activation parameters, and first-order dependence on $[\text{OH}^-]$ indicate that both nucleophilic attack and leaving group departure occur in the rate-determining step, consistent with a concerted $\text{A}_{\text{N}}\text{D}_{\text{N}}$ mechanism. The degree of bond formation to the nucleophile in the transition state is not given by the data collected in this study. The identity of the nucleophile is important, however, as seen from the dependence of the rate of hydrolysis on hydroxide concentration and the lack of an observable rate with the weaker nucleophile phenoxide.

Experimental Section

All chemicals and solvents were purchased from commercial sources and used without purification, unless otherwise noted. ^1H NMR spectra were recorded at 400 MHz in CDCl_3 relative to TMS (0.00 ppm). ^{13}C NMR spectra were recorded at 101 MHz (proton decoupled) in CDCl_3 relative to CDCl_3 (77.2 ppm). GC–MS parameters: column length, 30 m; ID number, 0.25; carrier gas, He; detector volts, 0.85 eV; electron impact volts; 0.70 eV. FTIR data were obtained from KBr pellets at 2.0 cm^{-1} resolution. HPLC column parameters: HASIL 100 C 18 $5\text{ }\mu\text{m}$ $250 \times 4.6\text{ mm}$.

Phenyl Sulfuryl Chloride (1). A modification of a literature method was used.³¹ A slurry of potassium phenoxide (9.7778 g, 0.074 mol) was added to a solution of distilled $\text{SO}_2\text{-Cl}_2$ (6.022 mL, 0.074 mol) in benzene at $0\text{ }^\circ\text{C}$ under N_2 over 30 min; a yellow solution and precipitate resulted. The solution was allowed to come to rt, filtered, and washed with water. The benzene layer was dried with MgSO_4 and the solvent removed under reduced pressure; a brown oil resulted. The oil was separated on silica gel (32–63 μm), eluting with hexane; a clear oil resulted. The oil was finally distilled at 19 mmHg, with collection done at $69\text{--}70\text{ }^\circ\text{C}$; a clear oil resulted (2.4162 g, 0.013 mol, 17% yield): $\text{C}_6\text{H}_5\text{ClO}_3\text{S}$ MW 192.62, d 1.39; ^1H NMR δ 5.88–6.01 (m).

4-Chloro-3-nitrophenyl Phenyl Sulfate (2). Compound **1** (0.67 mL, 0.005 mol) was added dropwise over 30 min to a solution of 4-chloro-3-nitrophenol (0.7701 g, 0.005 mol) and DBU (0.83 mL, 0.007 mol) in THF at rt under N_2 and left for 24 h. The solution was filtered and the solvent removed under reduced pressure. The resulting oil was suspended in CHCl_3 and precipitated with hexane; maroon crystals resulted. The crystals were filtered and washed with cold hexane and recrystallized (0.3361 g, 0.001 mol, 23% yield): $\text{C}_{12}\text{H}_8\text{ClNO}_6\text{S}$ MW 329.71; mp $81\text{--}83\text{ }^\circ\text{C}$; ^1H NMR δ 7.19 (s), 7.26 (d, 2H, $J = 8.1\text{ Hz}$), 7.33 (t, 1H, $J = 7.3\text{ Hz}$), 7.38–7.45 (m, 3H), 7.56 (d, 1H, $J = 8.9\text{ Hz}$), 7.75 (d, 1H, $J = 2.4\text{ Hz}$); ^{13}C NMR δ 119.2 (s), 121.1 (s), 126.3 (s), 128.4 (s), 130.6 (s), 133.6 (s); GCMS m/z (rel intensity) 329 (M^+ , 11), 183 (1), 172 (3), 155 (1) 142 (1), 128 (3), 126 (7), 107 (8), 100 (2), 98 (7), 93 (100), 65 (67); FTIR ν 1541 (vs), 1474 (s), 1424 (vs), 1356 (m), 1220 (s), 1186 (s), 1137 (s), 950 (m), 881 (vs), 846 (vs), 791 (s), 691 (m), 562 (s) cm^{-1} . Anal. Calcd for $\text{C}_{12}\text{H}_8\text{ClNO}_6\text{S}$: C, 43.71; H, 2.45; N, 4.25. Found: C, 43.80; H, 2.44; N, 4.34.

4-Nitrophenyl Phenyl Sulfate (3). Same procedure as for **2**. **1** (0.70 mL, 0.005 mol), 4-nitrophenol (0.6930 g, 0.005 mol), $\text{C}_{12}\text{H}_9\text{NO}_6\text{S}$ colorless crystals (0.2240 g, 0.001 mol, 15% yield): MW 295.27; mp $72\text{--}73\text{ }^\circ\text{C}$; ^1H NMR δ 7.19 (s), 7.25 (d, 2H, $J = 7.8\text{ Hz}$), 7.32 (t, 1H, $J = 7.3\text{ Hz}$), 7.41 (q, 4H, $J = 7.7\text{ Hz}$), 8.26 (d, 2H, $J = 9.0\text{ Hz}$); ^{13}C NMR δ 121.2 (s), 122.1 (s),

126.0 (s), 128.3 (s), 130.5 (s); GC–MS m/z (rel intensity) 295 (M^+ , 22), 215 (2), 187 (2), 129 (1), 108 (1), 93 (100), 65 (70); FTIR ν 1529 (s), 1483 (m), 1429 (s), 1348 (s), 1218 (m), 1177 (m), 1136 (s), 922 (m), 887 (vs), 785 (s), 690 (m), 554 (m) cm^{-1} . Anal. Calcd for $\text{C}_{12}\text{H}_9\text{NO}_6\text{S}$: C, 48.81; H, 3.07; N, 4.74. Found: C, 48.91; H, 3.08; N, 4.75.

2,6-Difluorophenyl Phenyl Sulfate (4). Same procedure as for **2**. **1** (0.60 mL, 0.004 mol), 2,6-difluorophenol (0.5403 g, 0.004 mol), $\text{C}_{12}\text{H}_8\text{F}_2\text{O}_4\text{S}$ colorless crystals (0.1070 g, 0.0004 mol, 9% yield): MW 286.25; mp $54\text{--}55\text{ }^\circ\text{C}$; ^1H NMR δ 5.52 (t, 2H, $J = 8.1\text{ Hz}$), 5.73–5.78 (m, 1H), 5.83–5.87 (m, 1H), 5.91–5.96 (m, 4H); ^{13}C NMR δ 112.8 (m), 113.1 (m), 128.0 (s), 128.6 (t, $J = 9\text{ Hz}$), 130.2 (s); GC–MS m/z (rel intensity) 286 (M^+ , 15), 206 (4), 194 (6), 178 (2), 165 (1), 146 (2), 129 (42), 93 (100), 65 (79); FTIR ν 1609 (w), 1497 (m), 1481 (m), 1421 (vs), 1250 (w), 1219 (m), 1182 (m), 1139 (m), 1015 (m), 880 (s), 786 (m), 769 (m), 691 (w), 552 (m), 531 (w) cm^{-1} . Anal. Calcd for $\text{C}_{12}\text{H}_8\text{F}_2\text{O}_4\text{S}$: C, 50.35; H, 2.82. Found: C, 50.58; H, 2.79.

2-Fluoro-4-nitrophenyl Phenyl Sulfate (5). Same procedure as for **2**. **1** (0.90 mL, 0.006 mol), 2-fluoro-4-nitrophenol (1.0068 g, 0.006 mol), $\text{C}_{12}\text{H}_8\text{FNO}_6\text{S}$ colorless crystals (0.1284 g, 0.0004 mol, 6.4% yield): MW 313.26; mp $49\text{--}50\text{ }^\circ\text{C}$; ^1H NMR δ 7.01 (s), 7.12–7.25 (m, 5H), 7.37 (t, 1H, $J = 8.3\text{ Hz}$), 7.86–7.89 (m, 2H); ^{13}C NMR δ 113.9 (d, $J = 23\text{ Hz}$), 120.6 (s), 121.2 (s), 124.2 (s), 128.4 (s), 130.5; GC–MS m/z (rel intensity) 313 (M^+ , 17), 233 (2), 221 (1), 205 (2), 133 (1), 126 (1), 110 (1), 93 (100), 65 (77); FTIR ν 1533 (s), 1487 (m), 1423 (vs), 1356 (m), 1263 (m), 1213 (m), 1167 (m), 1142 (m), 923 (m), 903 (m), 867 (m), 807 (vs), 786 (m), 703 (m), 687 (m), 579 (m), 557 (m) cm^{-1} . Anal. Calcd for $\text{C}_{12}\text{H}_8\text{FNO}_6\text{S}$: C, 46.01; H, 2.57; N, 4.47. Found: C, 46.00; H, 2.49; N, 4.47.

Pentafluorophenyl Phenyl Sulfate (6). Same procedure as for **2**. **1** (0.41 mL, 0.003 mol), pentafluorophenol (0.5390 g, 0.003 mol), $\text{C}_{12}\text{H}_5\text{F}_5\text{O}_4\text{S}$ colorless crystals (0.1511 g, 0.0004 mol, 15% yield): MW 340.22; mp $27\text{--}28\text{ }^\circ\text{C}$; ^1H NMR δ 5.75 (s, 1H), 5.88–5.99 (m, 4H); ^{13}C NMR δ 121.1 (s), 128.4 (s), 130.4 (s); GC–MS m/z (rel intensity) 340 (M^+ , 5), 183 (8), 155 (18), 117 (3), 105 (3), 93 (100), 65 (94); FTIR ν 1520 (vs), 1488 (w), 1433 (s), 1216 (m), 1133 (m), 998 (s), 917 (w), 893 (s), 796 (m), 779 (w), 561 (w). Anal. Calcd for $\text{C}_{12}\text{H}_5\text{F}_5\text{O}_4\text{S}$: C, 42.36; H, 1.48. Found: C, 42.41; H, 1.37.

3-Fluoro-4-nitrophenyl Phenyl Sulfate (7). Same procedure as for **2**. **1** (0.93 mL, 0.007 mol), 3-fluoro-4-nitrophenol (1.0340 g, 0.007 mol), $\text{C}_{12}\text{H}_8\text{FNO}_6\text{S}$ yellow crystals (0.4507 g, 0.001 mol, 22% yield): MW 313.26; mp $69\text{--}70\text{ }^\circ\text{C}$; ^1H NMR δ 7.19–7.26 (m, 3H), 7.33 (t, 1H, $J = 7.3\text{ Hz}$), 7.40 (t, 2H, $J = 7.6\text{ Hz}$), 8.10–8.13 (m, 2H); ^{13}C NMR δ 112.0 (d, $J = 25\text{ Hz}$), 117.4 (s), 121.1 (s), 128.1 (s), 128.5 (s), 130.6 (s); GC–MS m/z (rel intensity) 313 (M^+ , 19), 126 (1), 110 (1), 97 (1), 93 (100), 65 (80); FTIR ν 1617 (m), 1600 (m), 1534 (s), 1488 (m), 1418 (s), 1349 (m), 1261 (m), 1124 (m), 1091 (m), 971 (s), 891 (s), 816 (s), 785 (m), 558 (m) cm^{-1} . Anal. Calcd for $\text{C}_{12}\text{H}_8\text{FNO}_6\text{S}$: C, 46.01; H, 2.57; N, 4.47. Found: C, 46.08; H, 2.46; N, 4.45.

[^{15}N]-4-nitrophenyl [^{18}O]yl phenyl sulfate was prepared as described for compound (**3**): [^{14}N]-4-nitrophenol³² and [^{15}N]-4-nitrophenyl [^{18}O]ol were prepared as previously described²⁶ and mixed to closely reconstitute natural abundance nitrogen ($^{15}\text{N}/^{14}\text{N} = 0.365\%$). Mixed 4-nitrophenol (0.1579 g, 0.001 mol). Compound **1** (0.16 mL, 0.001 mol): $\text{C}_{12}\text{H}_9\text{NO}_6\text{S}$ (0.0748 g, 0.0003 mol, 22% yield).

^{18}O -Tracer Procedure. Compound **4** (10.6 mg, 0.037 mmol) was hydrolyzed in 500 μL of 1,4-dioxane and 500 μL of 1.0 N NaOH (32% H_2^{18}O) at $80\text{ }^\circ\text{C}$ for 4 h. The solution was neutralized with 500 μL of 4.0 N HCl. 2,6-Difluorophenol was extracted with 1.0 mL of diethyl ether (4 \times) and dried with MgSO_4 . The ether layer was concentrated to 300 μL and the incorporation of ^{18}O determined by GC–MS (see the Supporting Information). Excess ether was evaporated from the aqueous layer, and phenyl sulfate was precipitated as the

(31) Penney, C. L.; Perlin, A. S. *Carbohydr. Res.* **1981**, *93*, 241–246.

(32) Hengge, A. C.; Cleland, W. W. *J. Am. Chem. Soc.* **1991**, *113*, 5835–5841.

barium salt by addition of 200 μL of aqueous barium chloride (satd). This was then centrifuged and washed with 2.0 mL of the following: 4 N HCl (2 \times), water (3 \times), and ethanol (2 \times). Finally, barium phenyl sulfate was dried under reduced pressure at 100 $^{\circ}\text{C}$ for 1 day. Incorporation of ^{18}O was determined by FTIR (KBr pellet), and ^{18}O incorporation was assessed similar to the method of Spencer³³ (see the Supporting Information). A control experiment was done identically in unlabeled H_2O .

HPLC Procedure. Hydrolysis of compound **3** was followed by HPLC at 285 nm. Solutions of 33 μM in 0.5 N NaOH in 10% 1,4-dioxane were heated at 60 $^{\circ}\text{C}$ for 1, 2, and 3 half-lives. These were then neutralized with acid (pH < 2), the phenols were extracted with diethyl ether and dried with MgSO_4 , and the solvent was removed under reduced pressure. The residue was dissolved in 300 μL of 1:1 (v/v) acetonitrile/water (conc \approx 3 mM), and then 10 μL was injected into the HPLC, isocratic elution: 3.0 mL min^{-1} 4 mM glacial acetic acid/4 mM triethylamine buffer (pH 4.25) and 0.75 mL min^{-1} acetonitrile. 4-nitrophenol and phenol calibration standards were done at a total concentration of 2.5 mM with 4-nitrophenol/phenol ratios ranging from 95/5 to 80/20. Potassium phenyl sulfate was hydrolyzed and analyzed under identical conditions (except that of initial concentration; 100 μM) as a control.

Kinetics. The kinetics of compounds **2**–**7** at a concentration of 33 μM in a 3 mL sealed quartz cuvette were monitored spectrophotometrically (see the Supporting Information for wavelengths and kinetic data) with concentrations of 0.25, 0.50, 0.75, and 1.0 N NaOH 10% 1,4-dioxane at 40 $^{\circ}\text{C}$. Rate constants were obtained by a first-order fit to the full time courses for reaction. The second-order reaction rate constant k_{OH} for each diester was determined from the slope of the line of the first-order rate constants plotted as a dependent function of hydroxide concentration.

Activation Parameters. The kinetics of compounds **2** and **3** were monitored spectrophotometrically at 400 nm. Hydrolyses were done at a concentration of 33 μM in a 3 mL sealed quartz cuvette from 30 $^{\circ}\text{C}$ (303.15 $^{\circ}\text{K}$) to 60 $^{\circ}\text{C}$ (333.15 $^{\circ}\text{K}$) in 0.5 N NaOH 10% 1,4-dioxane (see the Supporting Information for kinetic data).

^{15}k KIE Procedure. Natural abundance compound **3** was partially hydrolyzed in 200 mL of 0.5 N NaOH 20% 1,4-dioxane at 40 $^{\circ}\text{C}$. The reaction was stopped by acidification to pH 2 with concentrated HCl, and the products were extracted with 150 mL of diethyl ether (3 \times). Before acidification, the percentage of reaction was monitored spectrophotometrically at 400 nm by measuring the absorbance of an aliquot of the mixture and then subjecting the aliquot (100 μL in 3.0 mL of 1.0 N

NaOH) to full hydrolysis followed by another spectrophotometric measurement at 400 nm. The organic layer of the main reaction mixture was dried over MgSO_4 and filtered and the solvent removed under reduced pressure. The residue was separated via preparative TLC (with a fluorescent indicator), solvent 1:1; hexane/diethyl ether. Recovered 4-nitrophenol ($R_f \approx 0.4$), following elution with diethyl ether and subsequent removal under reduced pressure, was sublimed under vacuum at 90 $^{\circ}\text{C}$. Recovered unreacted **3** ($R_f \approx 0.7$), following elution with diethyl ether, was further purified on a Chromatron (1 mm plate of silica gel 60 PF-254, solvent 4:1; hexane/diethyl ether); solvent was removed under reduced pressure. In a tin capsule (6 \times 4 mm), recovered 4-nitrophenol (\sim 1 mg) or recovered compound **3** (\sim 2 mg) was placed and sealed for isotopic ratio analysis using an ANCA-NT combustion system in tandem with a Europa 20-20 isotope ratio mass spectrometer. Each experiment was performed in triplicate, and each measurement agreed to within experimental error. Three samples of unreacted compound **3** (\sim 2 mg) were also analyzed.

$^{18}\text{k}_{\text{lg}}$ KIE Procedure. The $^{18}\text{k}_{\text{lg}}$ isotope effect was measured with a similar technique as described above for ^{15}k , using the mixture of [^{14}N] 4-nitrophenyl phenyl sulfate and [^{15}N] 4-nitrophenyl [^{18}O] phenyl sulfate. This method utilizes the remote label method³⁴ in which the isotope ratio of the nitrogen atom serves as a reporter for oxygen isotope ratios. The observed isotope effect was corrected for ^{15}k and for incomplete isotopic incorporation, as previously described.¹⁶

Acknowledgment. Financial support of this work came from USU URCO 2002 grant to J.M.Y., USU CAB 2002 grant to J.M.Y., and NIH 47297 grant to A.C.H. Acknowledgment is given to Shimadzu Instruments, Inc. (Columbia, MD), for use of the Shimadzu Analytical Sciences Laboratory at USU.

Supporting Information Available: ^{18}O -tracer GC-MS/FTIR spectra; kinetic data showing first-order dependence of hydrolysis rate on hydroxide concentration; kinetic data used for determination of activation parameters for the hydrolysis of (**2**) and (**3**); wavelengths and kinetic data used for determination of the second-order rate constants used for β_{lg} ; and amounts, equations, and isotopic incorporation data for ^{15}k and $^{18}\text{k}_{\text{lg}}$ KIE experiments. This material is available free of charge via the Internet at <http://pubs.acs.org>.

JO0488309

(33) Spencer, B. *Biochem. J.* **1959**, 73, 442–447.

(34) O'Leary, M. H.; Marlier, J. F. *J. Am. Chem. Soc.* **1979**, 101, 3300–3306.